# Electric Contact Material Selection for Medium and High Voltage DC Circuit Breakers

## Tushar Damle, Michael Varenberg & Lukas Graber

Transactions on Electrical and Electronic Materials

ISSN 1229-7607

Trans. Electr. Electron. Mater. DOI 10.1007/s42341-020-00180-5





Your article is protected by copyright and all rights are held exclusively by The Korean Institute of Electrical and Electronic Material **Engineers. This e-offprint is for personal** use only and shall not be self-archived in electronic repositories. If you wish to self-archive your article, please use the accepted manuscript version for posting on your own website. You may further deposit the accepted manuscript version in any repository, provided it is only made publicly available 12 months after official publication or later and provided acknowledgement is given to the original source of publication and a link is inserted to the published article on Springer's website. The link must be accompanied by the following text: "The final publication is available at link.springer.com".



Transactions on Electrical and Electronic Materials https://doi.org/10.1007/s42341-020-00180-5

Online ISSN 2092-7592 Print ISSN 1229-7607

#### **REGULAR PAPER**



### Electric Contact Material Selection for Medium and High Voltage DC Circuit Breakers

Tushar Damle<sup>1</sup> · Michael Varenberg<sup>2</sup> · Lukas Graber<sup>1</sup>

Received: 19 August 2019 / Revised: 21 January 2020 / Accepted: 14 February 2020 © The Korean Institute of Electrical and Electronic Material Engineers 2020

#### Abstract

Medium and high voltage DC grids are increasingly proposed for terrestrial, shipboard and aircraft power systems. However, multi terminal DC networks can only be realized with the development of a DC circuit breaker. Due to the difficulty in breaking DC currents, hybrid circuit breakers—which consist of a non-arcing fast mechanical disconnect switch (FMS) in parallel with a solid state switch—is the most promising solution. The stresses experienced by the electric contacts of FMS are different from those of AC and low voltage DC breakers and disconnect switches. The choice of contact material has a significant impact on the performance of the DC circuit breaker. The Ashby method is used to systematically identify the best suited contact materials by translating the requirements of FMS contacts into objectives and constraints and deriving material indices for each objective. Minimizing power loss, wear and overheating of contacts are identified as the key objectives. The results suggest that copper-based alloys and compounds are more suitable than silver based alloys and compounds and other contact materials.

 $\textbf{Keywords} \ \ Contact \ materials \cdot Electric \ contacts \cdot Fast \ mechanical \ disconnect \ switch \cdot \ Ultra \ fast \ disconnector \cdot \ Hybrid \ circuit \ breaker$ 

#### 1 Introduction

DC grids enable higher efficiency bulk power transmission over long distances, easier integration of renewable energy and lower costs. These advantages have led to DC power systems being increasingly proposed for terrestrial, shipboard and aircraft power systems [1, 2]. A key enabling technology for multi-terminal DC grids are medium and high voltage DC circuit breakers to isolate faulted sections and break fault currents [3]. Several attempts at building DC circuit breakers have been made but none are reliable and commercially viable at medium and high voltages. This is due to the difficulty in breaking fault currents without natural zero crossing with a switching speed of less than a few milliseconds. A promising solution is the hybrid circuit breaker (HCB), which combines the advantages of both mechanical

and solid state switching. Figure 1 shows a commonly used HCB topology [4]. The nominal current flows through the main path which consists of the Fast Mechanical Disconnect Switch (FMS) and the current commutation switch (CCS). The fault current is moved to the commutation path which consists of solid-state switches by first opening the CCS. The FMS is then opened at zero current without arcing. Finally, the solid-state switches in the commutation path breaks the fault current.

A key challenge is the design of the FMS with a rated current of up to a few kiloamperes and an opening time of a few milliseconds or less [5]. The FMS have electric contacts with large surface area to operate at the rated DC current without melting. The contacts must also be low in mass and volume for high switching speeds. The contacts are moved using high-speed actuators such as Thompson coils [6, 7] or piezoelectric actuators [8, 9], which result in lower contact forces compared to conventional AC circuit breakers [10]. The lower contact forces make the FMS more susceptible to fretting wear [11] than conventional disconnect switches, especially in applications such as electric ships and aircraft, which are more likely to expose the contacts to mechanical vibrations than in stationary applications. The smaller

Published online: 28 February 2020



<sup>☐</sup> Tushar Damle tdamle3@gatech.edu

School of Electrical and Computer Engineering, Georgia Institute of Technology, Atlanta, GA, USA

Woodruff School of Mechanical Engineering, Georgia Institute of Technology, Atlanta, GA, USA

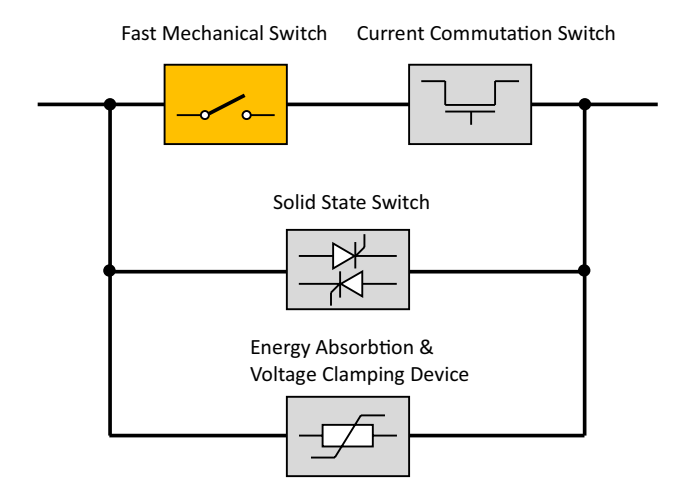
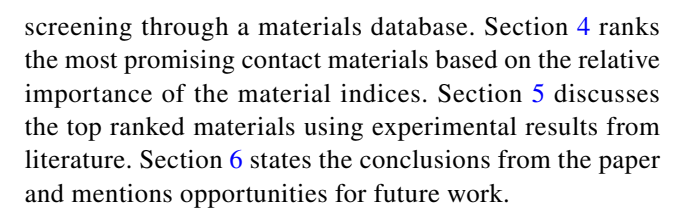


**Fig. 1** Typical hybrid circuit breaker topology with FMS (yellow). (Color figure online)

contacts also make them susceptible to overheating and melting due to increased thermal stress. Therefore, the contacts should be made of materials that combine high electrical and thermal conductivity with the ability to withstand wear and melting during normal and short circuit conditions. The material selection problem is very different from that of conventional AC breakers, which are design to withstand arcing but have switching speeds that are typically at least an order of magnitude lower than FMS.

In this paper, a systematic material selection approach known as the Ashby method [12] is used to identify and rank the most suitable contact materials for FMS. The desired performance features of the FMS, such as lower power loss, fretting wear and melting—are translated into objectives, constraints, and free variables, which are used to derive materials indices. A large database of materials is screened using the material indices to rank the most suitable contact materials for FMS. As the requirements for FMS contact materials are different from conventional circuit breakers, the work presented in this paper serves as the basis for future research in this area. As the FMS is a new type of switch in early stages of research, a systematic study to identify the best contact materials has yet not been performed. This paper identifies the best materials that will minimize power loss, wear and overheating. The top ranked materials are to be further investigated in the future through test data, analyses, availability, pricing, etc. to help to reduce the number of candidate materials to a level that is manageable for experimental validation.

This paper is divided into the following sections. Section 2 provides more technical background on the stresses experienced by FMS contacts, the material selection process and prior studies on this topic. In Sect. 3, the material indices are derived, and a trade-off chart is generated by



#### 2 Technical Background

The opening speed of DC breakers is determined by the rate of rise of fault current  $\frac{dI_f}{dt}$ . A high  $\frac{dI_f}{dt}$  would force substation and power equipment to be rated for higher short circuit withstand, which would greatly increase their size and cost. A fast switching breaker can clear the fault before the fault current reaches a high value.  $\frac{dI_f}{dt}$  is expected to be highest (worst case scenario) under a stiff source (no resistive losses) and bolted fault (low voltage drop at fault location), where it depends only on  $L_s$ , in which case

$$\frac{dI_f}{dt} = \frac{V_{dc}}{L_c} \tag{1}$$

where  $I_f$  is the magnitude of fault current,  $V_{dc}$  is the source voltage and  $L_s$  is the inductance of the source. In order to estimate the value of  $L_s$ , the main impact of such inductance on normal system operation needs to be considered, which is the transient voltage drop across that inductance during short circuit. This value will be limited to the maximum allowable rate of rise/fall of power  $dp_r/dt$  in pu/s. Another quantity required to determine  $L_s$  is the allowable sudden voltage drop  $dv_r$  when the DC system is exposed to such a high power ramp. If such a voltage drop is small (a well-regulated system), the maximum rate of rise of short circuit current is determined by

$$\frac{dI_f}{dt} = \frac{P_r}{V_r} \times \frac{dp_r}{dt} \times \frac{1}{dv_r}$$
 (2)

where  $P_r$  is the rated power of the DC system,  $V_r$  is the rated voltage of the system and  $dv_r$  is the voltage drop during fault as a fraction of  $V_r$ . A breaker with a fast opening time can not only significantly reduce the peak fault current level, but also the amount of energy produced by the fault current, which is absorbed by the devices in the system. This is particularly useful in medium voltage DC (MVDC) applications such as all electric ships and aircraft [13], where power density is very important and reducing the peak fault current can reduce the size of devices. To achieve multimegawatt MVDC systems, the rated voltages and currents are expected to be in the order of 12–24 kV and lower kiloamperes respectively [14]. A breaker rated 12 kV and 2 kA continuous current will have a rated power of



$$P_r = 12kV \times 2kA = 24MW \tag{3}$$

As there are no guiding standards for  $dp_r/dt$  in DC systems, we look at AC systems where a resistive load can be ramped up from zero to full power within a quarter cycle if connected to an AC source at the zero crossing of AC voltage. Hence, a DC system in which power can rise from zero to full power faster than that will probably be considered as very stiff. Assuming a relatively low  $dv_r = 2.5\%$ , and a relatively high  $\frac{dp_r}{dt} = 500 \, \text{pu/s}$ , (from zero to full power in 2 ms with only 2.5% voltage drop across  $L_s$ ), the rate of rise of fault current will not be higher than

$$\frac{dI_f}{dt} = \frac{24 \text{ MV}}{12 \text{ kV}} \times \frac{500 \text{ pu/s}}{\left(2.5/100\right)} = 40 \text{ A/\mu s}$$
 (4)

If the breaker clears the fault in 1.5 ms, this results in the fault current reaching a peak of

$$I_p = 40 \,\text{A/\mu s} \times 1500 \,\text{\mu s} = 60 \,\text{kA}$$
 (5)

This is comparable to the 63 kA fault current rating in 15 kV class AC breakers [15]. However, these breakers have an opening time of 3-5 cycles of AC current, which is an order of magnitude slower than the required opening time for MVDC applications. Hence, a drastically new design of circuit breakers is required for MVDC applications such as the Thomson coil and piezoelectric FMS in an HCB topology. The electric contacts must be designed to withstand the unique stress subject to the FMS. This includes selection of the electric contact material. The electric contacts of the FMS prototypes borrow from research on circuit breaker and vacuum interrupter contacts. SF<sub>6</sub> circuit breakers typically use contacts made of silver based refractory materials such as AgW, AgWC [16] and vacuum breakers typically use copper based contacts such as CuW and CuCr [17] contacts. However, the stresses experienced by contacts of FMS are different from the stresses on conventional breaker contacts. One key difference is that the FMS is non-arcing, so contact design considerations relating to change in geometry, resistance,

material erosion, and durability when exposed to repeated electric arcs, are no longer applicable. The contacts materials used in conventional circuit breaker may not necessarily be the best materials for the non-arcing FMS contacts.

Prior literature has focussed on selection of contact materials RF MEMS switches, AC circuit breakers and electrical connectors. Suitable materials have been identified based on the Ashby method, as well as other analytical and experimental methods. Table 1 summarizes the different applications and material selection methods used to identify suitable contact materials. The analytical methods include finite element analysis and other mathematical approaches to estimate the range of required material properties. The contact materials whose material properties are in this range are selected. The experimental methods conduct standardized tests on several materials and select the best materials based on the results. The analytical and experimental methods cannot be scaled to select the best material candidate among thousands of materials. They require a pre-screening step to reduce the number of candidate materials to a reasonable number. To select the best material for a new application, it is necessary to cast a wide net to not overlook new or unlikely material candidates. Methods such as the Ashby, VIKOR and TOPSIS [18] are used to screen and select the promising materials solution when there are multiple and conflicting objectives from a large database of materials. As the criteria for selecting electric contact material for FMS are multiple and conflicting, the Ashby method is used in this paper.

According to the Ashby method, the performance of a material for any engineering application is given by its performance index

$$P = f(F, G, M) \tag{6}$$

where f is the function of Functional (F), Geometric (G) and Material (M) parameters. These parameters are independent of each other and the overall performance of the materials depends on the collective output of individual parameters. The performance of the material can be maximized for all

**Table 1** Electric contact material selection approaches for different applications

Author	Electric contact application	Material selection method
Buggy and Conlon [19]	Electrical connectors	Analytical
Heitzinger et al. [17]	Vacuum interrupters	Analytical + experimental
Frey et al. [20]	Vacuum interrupters	Experimental
Watkins [21]	High power switches in EM Launchers	Ashby method
Amft [22]	Low voltage contactors	Analytical
Coutu et al. [23]	MEMS switches	Analytical
Sawant et al. [24]	RF MEMS switches	Ashby method + experiment
Deshmukh and Angira [25]	RF MEMS switches	Ashby, TOPSIS and VIKOR method



F and G by optimizing the material parameters or material index. The four steps of the Ashby method are:

- 1. Translate the design requirements as objectives, function, constraints, and free variables.
- 2. Screen the materials using constraints by eliminating materials that do not satisfy design requirements.
- 3. Rank the materials using objectives.
- 4. Seek supporting information by a detailed study of the top ranked materials.

The material selection is performed on all 3985 materials in the Level 3 CES database [26]. Only the first three steps of the Ashby method are used to identify the best materials for FMS, as this is a more general selection process. The fourth step, seeking documentation, involves further investigation of the top ranked candidates through familiarity of typical applications, failure modes, test data, analyses, availability, pricing, etc. to help thin out the list to one or two solutions. The material selection problem is a multi-objective optimization problem and Pareto optimization technique is used to identify suitable materials [27]. The Pareto optimal solution is a set of all non-dominated solutions from a given solution space. The non-dominated solutions are identified using tradeoff plots. In the tradeoff plots, the inverse of the material indices for each objective is plotted for better visualization. That is, the lower the value of the objective, the more viable the material. A Pareto optimal solution based on assigning weights to different objectives will be required to identify the most suitable material.

#### 3 Material Selection

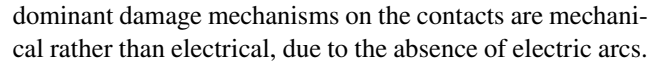
#### 3.1 Translation Table

FMS generally have a pair of contacts, which are identical in geometry and material. While the contacts of FMS can have different geometries to minimize electric field and contact resistance [28, 29], this analysis is meant to be independent of the geometry of the contact material.

The most important features of the electrical contact materials are:

- 1. Low power loss
- 2. High wear resistance
- 3. High resistance to overheating during short circuit

The contact material should also have a high work function to minimize breakdown by field emission. However, the work function of all commonly used contact materials (conductive metals and alloys) are in the similar (4–6 eV), so it is not considered in the material selection process. Also, the



With this information, the material selection problem can be set up as a multiple objective problem. The translation table is shown in Table 2.

#### 3.2 Material Indices

The first objective is to minimize the power loss P in the contacts, which is expressed as  $P = I_0^2 R$ , where  $I_0$  nominal current through the FMS and R is the resistance of the contact pair. The contact resistance R is a function of the resistivity, geometry, surface roughness and contact force. The force between contacts is specified for a given type of FMS. Also, it is assumed that the materials considered can all be machined to any desired surface roughness so the effect of the real area of contact between a contact pair can be neglected. While there is no general formula for the resistance on an arbitrary geometry, it is clear that the resistance is directly proportional to the resistivity of the material.

$$R = C \cdot \rho_c \tag{7}$$

where  $\rho_c$  is he resistivity of the material, and C is the constant of proportionality that depends on the geometry. Substituting the equation for resistance in the objective equation, we get

$$P = CI_0^2 \rho_c \tag{8}$$

Since the current through the contacts is specified and the analysis is independent of the geometry of the contact, the material index is

$$M_1 = \rho_c \tag{9}$$

which is to be minimized.

The second objective is to minimize wear experienced by contacts. The contacts experience electrical, mechanical and thermal stresses which lead to different types of wear.

Table 2 Translation table

Function	Light-conductive-wear resistant contact material
Objective	Minimize power loss (during normal operation) Minimize wear Minimize contact overheating (during fault)
Constraints	Good electric conductor ( $<10~\mu\Omega$ cm) Good thermal conductor ( $>173~W/mK$ ) High hardness ( $>100~HV$ ) The force between the contacts is specified. The current carried by the contacts is specified. The dimensions (length/radius, area of contact) of the electric contacts are specified.
Free variables	Choice of material



The wear types experienced by the contacts according to the classification in [30] are:

- 1. Fretting wear due to micro-slips at the contact interface
- 2. Impact wear due to closing of contacts at high speed

The fretting wear is caused by micro-slips at the interface of the contacts due to mechanical vibrations, thermal expansion and electrodynamic forces. Studies have shown that fretting wear depends on the fretting frequency, current load normal force, slip amplitude and temperature of the contacts [31]. The contact resistance has been shown to increase by at least an order of magnitude after the onset of fretting damage. The number of cycles to failure by fretting has been shown to be lower under higher thermal stress [32], which is expected in all FMS and lower contact force [33], which is expected in piezoelectric FMS. This is the most dominant wear mechanism capable of causing most damage. The FMS is also subject to impact wear when the contacts close at high speed. The FMS, like most circuit breakers and vacuum interrupters, is expected to be rated for 20,000 operations and have a lifetime of 20 years. This means about 1000 operations per year on average. The low number of expected switching operations make impact wear the less dominant wear mechanism.

Fretting wear follows the Archard's wear equation which is given by

$$Q = K \frac{NL}{H} \tag{10}$$

where Q is the volume of wear debris, K is the dimensionless wear coefficient, L is the sliding distance, N is the force between the contacts and H is the hardness the material. In the case of fretting, the sliding distance L is proportional to the amplitude of micro-slip at the interface of the contacts, which is, in turn, proportional to the contact stiffness (can be represented as Young's modulus, E), and is inversely proportional to load N [34].

The dimensionless wear coefficient K is defined as the probability of each asperity interaction resulting in the production of a wear particle. K depends on the material properties, geometry of the contact zone, surface roughness and testing conditions and the exact value of K is not available for many candidate contact materials under uniform conditions. Considering the unavailability of K for all the candidate materials, the second material index is assumed to be

$$M_2 = \frac{E}{H} \tag{11}$$

which is to be minimized

The impact wear of contact surfaces, while not being the dominant wear mechanism, is also thought to decrease with decreasing  $M_2$ . Increasing hardness leads to increase in

material strength, and, hence, to decrease of surface damage. Decreasing Young's modulus leads to increase in material compliance, and, hence, to an accommodation of impact energy through elastic deformation rather than through interfacial slip and generation of structural defects. Thus, the material index  $M_2$  covers both fretting and impact wear.

The third objective is to minimize overheating of contacts during short circuit, which can cause the contacts to melt and/or weld together. The contacts are susceptible to overheating when there is rapid rise in current due to a fault. Based on the current interruption process of HCB in Fig. 1, the contacts of the FMS are exposed to fault current until the current commutation switch opens and moves the current to the semiconductor branch. Therefore, the heat energy produced by the fault is assumed to be

$$E_{in} = \int_{0}^{t} I_f^2(t)R(t)dt \tag{12}$$

where  $E_{in}$  is the heat energy produced by the fault,  $I_f$  is the instantaneous fault current across the FMS, R is the contact resistance and t is the time between the inception of the fault and commutation. The energy produced can be assumed to be not greater than

$$E_{in} \cong I_p^2 Rt \tag{13}$$

where  $I_p$  is the peak fault current rating of the FMS, which is specified. The material index is derived through the energy balance equation given by

$$E_{in} = E_{out} + E_{absorbed} \tag{14}$$

where  $E_{out}$  is the heat energy removed by conduction and  $E_{absorbed}$  is the heat energy absorbed by the contacts, which causes overheating. Due to rapid rise of heat and short time duration of faults, it is assumed that there is insufficient time to conduct heat away from the contacts. The thermal energy stored in the contacts is given by

$$E_{absorbed} = \rho V C_p \Delta T \tag{15}$$

where  $\rho$  is the density of the contact material, V is the volume,  $C_p$  is the heat capacity and  $\Delta T$  is the rise in temperature. The equations for  $E_{in}$  and  $E_{absorbed}$  are equated which results in

$$\Delta T = \frac{I_p^2 Rt}{\rho V C_p} \tag{16}$$

The impact of the rise in temperature is material dependent. A material with a high melting point exposed to the same temperature will not cause the same amount of surface damage as a material with a lower melting point.



So  $\Delta T$  is normalized by the melting temperature  $T_{melt}$  to give homologous temperature rise

$$\frac{\Delta T}{T_{melt}} = \frac{I_P^2 Rt}{\rho V C_p T_{melt}} = \frac{I_P^2 C \rho_c t}{\rho V C_p T_{melt}}$$
(17)

The third material index is therefore given by

$$M_3 = \frac{\rho_c}{\rho C_p T_{melt}} \tag{18}$$

which is to be minimized. Considering that  $M_1$  is part of  $M_3$ , we can proceed to further analysis based on material indices  $M_2$  and  $M_3$  only.

#### 3.3 Material Database

The material property charts are created using the CES Edupack Level 3 database. The Level 3 database consists of materials that cover the major engineering material families (metals, ceramics, glasses, polymers, elastomers and hybrids) so new or unlikely opportunities are not overlooked. However, the database does not contain commercial materials such as AgWC, AgW, and CuW, which are currently used as electric contacts for conventional circuit breakers and vacuum interrupters. An analysis of contact materials for FMS would not be complete without including these materials. These contact materials are added to the CES database using the 'Add Record' feature of CES. The materials properties such as resistivity, density and hardness are available by manufacturer datasheets [35]. Other properties, such as heat capacity, thermal conductivity and tensile and compressive strengths are estimated using the "Hybrid Synthesizer" feature of CES. The hybrid synthesizer predicts the properties of hybrid materials such as sandwiches, foams, lattices and composites. The commercial contacts materials not available in CES are particulate metal matrix composites, the properties of which can be predicted by the Hybrid Synthesizer if the matrix, particulate material and volume fraction of the particulate material are specified.

This results in a database of about 4000 materials. To further reduce the subset, some reasonable assumptions about the material properties are made which are added as limit stages. These are:

- The material has a solid bulk form, which includes plates, bars, rods, forging, casting, extrusion and molding.
- 2. Electrical Resistivity < 10  $\mu\Omega$  cm (Resistivity of Iron, which is not a good contact material due to low electrical conductivity)
- 3. Hardness > 100 Vickers



4. Thermal conductivity > 173 W/mK ( $\lambda$  of Tungsten, which is also not a good contact material due to poor thermal conductivity)

This limits the subset of materials to 95, which is a much more manageable number.

#### 3.4 Material Property Charts

The material selection involves three objectives: minimizing power loss, minimizing wear and minimizing overheating. This multi-objective selection problem is addressed by generating tradeoff plots for the material indices against each other. Since the material index  $M_3$  includes  $M_1$ , only the tradeoff plot for  $M_2$  versus  $M_3$  is generated. The tradeoff plots, also known as material property charts, are plotted on the logarithmic scale for visualization purpose. The materials are represented by circles or ovals on the plot which shows a range of material property values for the given objectives. The white ovals represent materials in the CES database and the black ovals represent materials added to the database (AgW, AgWC, CuW) with the 'Add Record' feature of CES. The tradeoff surface is represented by the dotted curve. The ideal material solution should be found on the bottom left corner of the charts. If no material solution exists in this region then the materials near the tradeoff surface offer the best compromises.

Figure 2 shows the tradeoff plot for  $M_2$  versus  $M_3$ . Materials close to the tradeoff curve and other well-known materials are labelled. It also shows that contact materials such as AgWC, AgW and CuW, which were added to the database CES database, do not lie in the bottom left of the curves, indicating that these are not the best contact materials for FMS. The large gap in the bottom left area indicates that there is no ideal material solution. However, it is possible to rank the contact materials based on the relative importance of the performance indices.

#### 4 Material Ranking

The ranking of the materials can be accomplished by weighing the relative performance of each material index shown:

$$W_i = w_i \frac{(M_i)\min}{M_i} \tag{19}$$

where  $w_i$  is a weight factors which sum up to 1,  $M_i$  is the material index value, and  $(M_i)min$  is the minimum material index value of the materials that pass the screening stage. This results in two weighted values  $W_i$  for each of the selected materials. The summation of the two weighted values is the overall performance P of each material candidate:

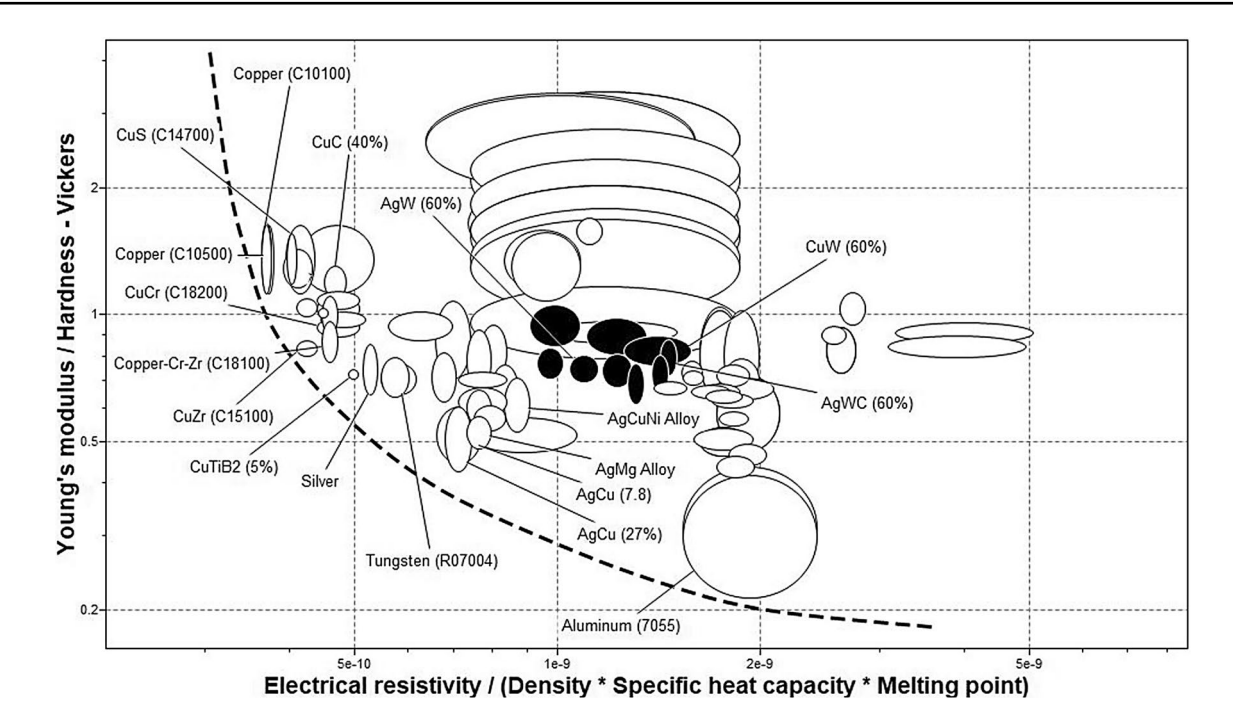


Fig. 2 Tradeoff plot for minimizing wear damage versus minimizing overheating

$$P = \sum W_i \tag{20}$$

The weight factors  $w_1$  and  $w_2$  correspond to  $M_2$  and  $M_3$  respectively. The weight factors are selected based on perceived importance of each material index to the performance of electric contacts of FMS. Since there are no commercially available FMS, the overall performance is used to rank the material candidates to develop a list of candidates to be pursued further with the understanding that the candidates are based on the current knowledge of operating conditions of FMS and that they may change as knowledge improves.

Table 3 shows the materials ranked from high to low based on each material index. The purpose of this table is to gain more insight into different materials that can be used as electric contacts based on relative weights given to different objectives. For each of the representative candidates listed in Table 2 several alloys, heat treatments and mechanical processing would be used to refine the selection for each class of material. For example, over a dozen different types copper pass the screening process.

However, the purpose of this exercise was is to establish a baseline of different material candidates for relative comparison. For this reason, the candidates are listed in Table 2 with the understanding that a wide range of properties may be obtained from alloying, heat treatment, or work hardening to meet more specific needs that are explored in the fourth step, documentation Therefore, variation of the same material such as Copper 10500, Copper 10200 have all been represented by Cu, and CuW (70% Cu), CuW (60% Cu), CuW (50% Cu) have all been represented by CuW.

The table shows that if minimizing power loss is the main objective, then materials such as Ag, Cu and silver and copper based alloys are the most suitable materials. If minimizing wear is the main objective, then aluminum, silver and silver-based alloys are more suitable. If minimizing overheating is the main objective, then copper and copper-based alloys are most suitable.

In this paper, the material ranking is shown for three cases. Minimizing wear and overheating are given equal importance in the first case, minimizing wear is given higher

**Table 3** Material ranking based on each objective

Objective (minimize)	Metric	Material ranking (high-low)
Power loss	$ ho_c$	Ag, Cu, CuTe, CuS, AgCu, CuC, CuZr, CuCr
Wear	$\frac{E}{H}$	Al, AgCu, Ag, CuPd, AgMg, AgCuNi, CuBeCo, Ag–MgO–NiO
Overheating	$rac{ ho_c}{ ho C_p T_{melt}}$	Cu, CuTe, CuS, CuZr, CuTr, CuTiB2, CuCd, CuC



relative importance in the second case and lower relative importance in the third case, and what is expected to be the most realistic case.

Case 
$$1 w_1 = 0.5, w_2 = 0.5$$

Table 4 shows the performance index of the highest ranked materials. copper, aluminum, copper-based alloys and silver have the highest performance index. This is likely not a realistic representation of relative performance of performance indices and is only shown for the purpose of illustration of the ranking procedure.

Case 
$$2 w_1 = 0.8, w_2 = 0.2$$

Table 5 shows the performance index of the highest ranked materials. Aluminum has the highest performance index followed by silver and copper-based alloys and tungsten. If minimizing wear in the contacts of the FMS is very high priority, then these materials would be most suitable as electric contacts.

Case 
$$3 w_1 = 0.2, w_2 = 0.8$$

While studies have shown higher fretting wear at lower contact force and elevated temperatures, the effect of current load on fretting is not clear. While some studies have shown that the onset of fretting is delayed by increasing current load, the currents in these experiments less than 3A [36, 37], which is too low to increase temperature of the contacts. At this time, it is unclear how a current load of a few hundred amperes or more affects fretting wear. However, materials with a high  $M_3$  are more resistant to surface damage caused by elevated temperatures. So we can assume a lower weight factor for  $M_2$  than  $M_3$ . This is considered to be the most realistic case based on current knowledge. Table 6 shows the performance index of the highest ranked materials. Copper and copper-based compounds and alloys have the best performance index. If minimizing overheating contacts of the FMS (and resistivity) is very high priority, then these materials would be most suitable as electric contacts.

Table 4 Weighted material ranking for case 1

Material	$M_2^{\rm a}$	$M_3  (\mu \Omega  \text{cm J}^{-1}  \text{kg}^{-1}  \text{m}^3)$	P
Cu	1.38	$3.69 \times 10^{-10}$	0.614
Al	0.3155	$1.97 \times 10^{-9}$	0.593
$CuTiB_2$	0.726	$4.975 \times 10^{-10}$	0.588
CuZr	1.042	$4.24 \times 10^{-10}$	0.586
CuCrZr	0.8715	$4.59 \times 10^{-10}$	0.582
CuS	1.37	$4.025 \times 10^{-10}$	0.573
AgCu	0.5165	$7.12 \times 10^{-10}$	0.564
Ag (99.9% purity)	0.571	$5.27 \times 10^{-10}$	0.56

 $<sup>^{</sup>a}M_{2}$  has no units shown in the table as is contains hardness H which is measured in the Vickers Scale (HV 10)



Material	$M_2^{\mathrm{a}}$	$M_3  (\mu \Omega  \text{cm J}^{-1}  \text{kg}^{-1}  \text{m}^3)$	P
Al	0.3155	$1.97 \times 10^{-9}$	0.837
Ag (coin silver)	0.5275	$7.14 \times 10^{-10}$	0.581
AgMg	0.531	$7.65 \times 10^{-10}$	0.572
CuPd	0.524	$9.01 \times 10^{-10}$	0.563
$CuTiB_2$	0.726	$4.975 \times 10^{-10}$	0.496
AgCuNi	0.6125	$8.7 \times 10^{-10}$	0.492
W	0.7085	$5.81 \times 10^{-10}$	0.483
CuZr	1.042	$4.24 \times 10^{-10}$	0.476

 $<sup>^{\</sup>mathrm{a}}M_{\mathrm{2}}$  has no units shown in the table as is contains hardness H which is measured in the Vickers Scale (HV 10)

#### 5 Discussion

The tradeoff plot shows that there is no materials available in the optimum region that meets all the objectives. Silver and copper-based materials were found to be more suitable materials than commercially available metal matrix composites that were added to the database. This can be explained by the fact that electric contacts of FMS have different requirements than conventional circuit breakers and switches. The contact materials were ranked based on best performance for each objective. The selection of the contact material would depend on relative weight assigned to each of these objectives.

Due to the large number of materials and varied tests required to test each objective, it is not possible to experimentally validate the material ranking for all the top ranked materials. However, experimental results in prior literature can be used to validate the ranking of materials. According to [38], the materials with lowest contact resistance are Au, Ag, AuPd, Cu and Cu alloys. However, Au and AgPd are screened out by the Ashby method due to low hardness. As a result, the top ranked materials for minimizing power loss

Table 6 Weighted material ranking for case 3

Material	$M_2^{\mathrm{a}}$	$M_3  (\mu \Omega  \text{cm J}^{-1}  \text{kg}^{-1}  \text{m}^3)$	P
Cu	1.38	$3.69 \times 10^{-10}$	0.845
CuS	1.37	$4.025 \times 10^{-10}$	0.779
CuZr	1.042	$4.24 \times 10^{-10}$	0.771
CuTe	1.295	$4.12 \times 10^{-10}$	0.765
$CuTiB_2$	0.726	$4.975 \times 10^{-10}$	0.719
CuCrZr	0.8715	$4.59 \times 10^{-10}$	0.715
CuCr	0.9365	$4.7351 \times 10^{-10}$	0.691
CuC	1.2	$4.675 \times 10^{-10}$	0.684

 $<sup>^{</sup>a}M_{2}$  has no units shown in the table as is contains hardness H which is measured in the Vickers Scale (HV 10)



in Table 3 fit well with the results from [38]. [39] shows that worn volume after fretting wear is lower in base metals than alloys due to faster oxidation in base metals. This tracks wells with Table 5 which has Al and Ag ranked the highest. [40] shows that fretting wear is lower in Al compared to Cu at low oscillation frequencies (0.33 Hz) and contact forces (2–10 N). This could explain the absence of Cu among the top ranked materials in Table 5. McDowell [41] and Beloufa [42] shows that fretting wear in copper alloys such as CuZr and CuPd is lower than pure Cu due to the higher hardness of copper alloys, which is also reflected in Table 5. There is no prior work on the comparative performance of fault current induced overheating/melting of silver and copper materials under identical conditions. However, [17, 43] and show that silver and copper have higher resistance to overheating than their alloys and metal based compounds respectively. As the specific heat capacity of copper based materials are higher than silver based materials [35], silver based materials heat up quickly and are more susceptible to overheating. That explains why Table 6 is dominated by copper based materials.

In summary, the ranking of materials in Tables 3 and 4 is broadly in agreement with experimental results. However, experimental data on every single material in the aforementioned tables cannot be found in literature. The broad agreement of experimental results with the material ranking from the Ashby method indicates that the top ranked materials must be investigated further with tests under identical conditions to find the most suitable contact material.

#### **6 Conclusions and Future Work**

The HCB is designed to limit fault currents and energy absorbed in DC power systems. This is accomplished by having nominal current flow through the FMS and commutating the fault current to the parallel solid state branch. The contacts of FMS must carry high continuous current with low power losses and must resist wear due to fretting, impact and Joule heating of contacts. The Ashby method is used to systematically identify the best suited contact materials by translating the requirements of contact materials into objectives and constraints and deriving material indices for each objective. CES Edupack was used to filter materials by applying constraints and rank materials using objectives. Commercially available metal matrix composite contact materials that were not in the CES database were added to make the analysis more thorough.

The results show that aluminum, silver and copper-based materials are the best materials if minimizing wear has high priority. Copper, aluminum and copper-based materials are the best materials if minimizing wear and overheating have equal priority. Copper-based materials are the best materials

if minimizing overheating (and power loss) has a high priority. Copper-based materials rank highly in all the cases shown, and the top 8 materials in the most realistic case are all copper-based. Therefore, copper based materials are more suitable as FMS contacts than silver based materials and any other material considered in this study. The top ranked materials must be investigated further by seeking further documentation of availability, pricing and conducting field tests under identical conditions to identify the most suitable material amongst them.

The analysis in this paper assumed that the dimensionless wear coefficient will have a minimal effect on the suitability to FMS for the top candidate materials. This needs to be validated by experimentally determining K for the top candidate materials. Also, the analysis assumed that the pair of contacts are made of the same materials. Commercial circuit breakers generally use contact pairs with the same materials so there is insufficient information on performance of dissimilar material contacts. However, there could be advantages to having contacts made of dissimilar materials as they have lower tendency to stick and could reduce wear. Also, electric contacts can be made of layers of different materials that have different desirable properties. These graded contacts can lead to better performance than contacts made of the same materials [44]. The feasibility of selecting most suitable materials in a system with dissimilar and graded contacts needs to be studied.

**Acknowledgements** This work was supported in part by the National Science Foundation through the Grant No. 1700887.

#### References

- V. Lenz, DC Current Breaking Solutions in HVDC Applications (ETH Zürich, Zürich, 2015)
- N. Doerry, J. Amy, The road to MVDC, in ASNE Intelligent Ships Symposium, 2015, pp. 20–21
- C.M. Franck, HVDC circuit breakers: a review identifying future research needs. IEEE Trans. Power Deliv. 26(2), 998–1007 (2011)
- M. Callavik, A. Blomberg, J. Häfner, B. Jacobson, The hybrid HVDC breaker. ABB Grid Syst. Tech. Pap. 361, 143–152 (2012)
- X. Pei, O. Cwikowski, D. Vilchis-Rodriguez, M. Barnes, A. Smith, R. Shuttleworth, A review of technologies for MVDC circuit breakers, in *IECON 2016-42nd Annual Conference of the IEEE Industrial Electronics Society* (IEEE, 2016), pp. 3799–3805
- C. Peng, I. Husain, A.Q. Huang, Evaluation of design variables in Thompson coil based operating mechanisms for ultra-fast opening in hybrid AC and DC circuit breakers, in *Applied Power Elec*tronics Conference and Exposition (APEC) (IEEE, 2015), pp. 2325–2332
- W. Wen et al., Research on operating mechanism for ultra-fast 40.5-kV vacuum switches. IEEE Trans. Power Deliv. 30(6), 2553– 2560 (2015)
- 8. M. Bosworth, D. Soto, R. Agarwal, M. Steurer, T. Damle, L. Graber, High speed disconnect switch with piezoelectric actuator



- for medium voltage direct current grids, in 2017 IEEE Electric Ship Technologies Symposium (ESTS) (IEEE, 2017), pp. 419–423
- K. Yasuoka et al., Arcless current interruption of DC 150A using a hybrid DC circuit breaker consisting of SiC-MOSFET and metal contacts, in *International Conference on Renewable Energies* and Power Quality, vol. 1 (2018). https://doi.org/10.24084/repqj 16.266
- C. Xu, T. Damle, L. Graber, A survey on mechanical switches for hybrid circuit breakers, in *Presented at the IEEE Power and Energy Society General Meeting*, Atlanta, GA USA, 2019
- X. Liu, Z. Cai, S. Liu, S. Wu, M. Zhu, Influence of wear test parameters on the electrical contact performance of brass alloy/ copper contactors under fretting wear. J. Mater. Eng. Perform. 28(2), 817–827 (2019)
- 12. M.F. Ashby, *Materials Selection in Mechanical Design* (Elsevier Science, Amsterdam, 2011)
- N. Doerry, J. Amy, The road to MVDC, in ASNE Intelligent Ships Symposium 2015
- Y. Khersonsky et al., Recommended Practice for 1 to 35 kV Medium Voltage DC Power Systems on Ships, 2010
- IEEE Standard for AC High-Voltage Circuit Breakers Rated on a Symmetrical Current Basis—Preferred Ratings and Related Required Capabilities for Voltages Above 1000 V. IEEE Std C37.06-2009, pp. 1–46. https://doi.org/10.1109/ieees td.2009.5318709
- V. Behrens, T. Honig, A. Kraus, E. Mahle, R. Michal, K. Saeger, Test results of different silver/graphite contact materials in regard to applications in circuit breakers, in *Proceedings of the Forty-First IEEE HOLM Conference on Electrical Contacts* (IEEE, 1995), pp. 393–397
- F. Heitzinger, H. Kippenberg, K. Saeger, K.-H. Schroder, Contact materials for vacuum switching devices. IEEE Trans. Plasma Sci. 21(5), 447–453 (1993)
- S. Opricovic, G.-H. Tzeng, Compromise solution by MCDM methods: a comparative analysis of VIKOR and TOPSIS. Eur. J. Oper. Res. 156(2), 445–455 (2004)
- M. Buggy, C. Conlon, Material selection in the design of electrical connectors. J. Mater. Process. Technol. 153, 213–218 (2004)
- P. Frey, N. Klink, R. Michal, K.E. Saeger, Metallurgical aspects of contact materials for vacuum switching devices. IEEE Trans. Plasma Sci. 17(5), 734–740 (1989)
- B.G. Watkins, Materials Selection and Evaluation of Cu-W Particulate Composites for Extreme Electrical Contacts (Georgia Institute of Technology, Atlanta, 2011)
- D. Amft, Selection of the contact material for low-voltage contactors, in *Proceedings of 17th International Symposium on Discharges and Electrical Insulation in Vacuum*, vol. 2 (IEEE, 1996), pp. 732–736
- R.A. Coutu Jr., P.E. Kladitis, K.D. Leedy, R.L. Crane, Selecting metal alloy electric contact materials for MEMS switches. J. Micromech. Microeng. 14(8), 1157 (2004)
- V.B. Sawant, S.S. Mohite, L.N. Cheulkar, Comprehensive contact material selection approach for RF MEMS switch. Mater. Today Proc. 5(4), 10704–10711 (2018)
- D. Deshmukh, M. Angira, Investigation on switching structure material selection for RF-MEMS shunt capacitive switches using Ashby, TOPSIS and VIKOR. Trans. Electr. Electron. Mater. 20(3), 181–188 (2019)

- C. EduPack, Granta Design Ltd, Cambridge UK, 2016. www.grant adesign.com/education
- V. Pareto, Manuale di economia politica (Societa Editrice, Milano, 1906)
- G.C. Lim, T. Damle, L. Graber, Optimized contact geometries for high speed disconnect switches, in 2017 IEEE Conference on Electrical Insulation and Dielectric Phenomenon (CEIDP) (IEEE, 2017), pp. 537–542
- L.G. Tushar Damle, Theoretical and experimental work on optimal contact geometries for fast mechanical disconnect switches, in *IEEE HOLM Conference on Electrical Contacts*, Albuquerque, NM, USA, 2018, vol. 64, 2018, pp. 24–30
- 30. M. Varenberg, Towards a unified classification of wear. Friction 1(4), 333–340 (2013)
- 31. M. Braunovic, Fretting in electrical/electronic connections: a review. IEICE Trans. Electron. **92**(8), 982–991 (2009)
- A. Lee, A. Mao, M. Mamrick, Fretting corrosion of tin at elevated temperatures, in *Proceedings of the Thirty Fourth Meeting of the IEEE Holm Conference on Electrical Contacts* (IEEE, 1988), pp. 87–91
- M. Braunovic, Effect of contact load on the contact resistance behaviour of different conductor and contact materials under fretting conditions, in *Proceedings of 19th ICEC*, Nuremberg, 1998, pp. 283–287
- M. Varenberg, I. Etsion, G. Halperin, Slip index: a new unified approach to fretting. Tribol. Lett. 17(3), 569–573 (2004). https://doi.org/10.1023/B:Tril.0000044506.98760.F9. (in English)
- 35. E. Vinaricky, G. Horn, V. Behrens, *Doduco Data Book of Electrical Contact*, New edn. (Doduco GmbH, Pforzheim, 2010)
- Y.W. Park, G.R. Bapu, K.Y. Lee, The influence of current load on fretting of electrical contacts. Tribol. Int. 42(5), 682–689 (2009)
- W. Ren, P. Wang, J. Song, G. Zhai, Effects of current load on wear and fretting corrosion of gold-plated electrical contacts. Tribol. Int. 70, 75–82 (2014)
- M. Antler, Field studies of contact materials: contact resistance behavior of some base and noble metals. IEEE Trans. Compon. Hybrids Manuf. Technol. 5(3), 301–307 (1982)
- 39. M. Antler, Electrical effects of fretting connector contact materials: a review. Wear **106**(1–3), 5–33 (1985)
- M. Braunovic, Degradation of Al–Al and Al–Cu connections due to fretting. Wear 125(1–2), 53–66 (1988)
- J. McDowell, Fretting corrosion tendencies of several combinations of materials, in *Symposium on Fretting Corrosion* (ASTM International, 1952)
- A. Beloufa, Conduction degradation by fretting corrosion phenomena for contact samples made of high-copper alloys. Tribol. Int. 43(11), 2110–2119 (2010)
- P.G. Slade, The current level to weld closed contacts, in 2013 IEEE 59th Holm Conference on Electrical Contacts (Holm 2013) (IEEE, 2013), pp. 1–7
- 44. S. Suresh, Graded materials for resistance to contact deformation and damage. Science **292**(5526), 2447–2451 (2001)

**Publisher's Note** Springer Nature remains neutral with regard to jurisdictional claims in published maps and institutional affiliations.

